Supporting Information

Marolt et al. 10.1073/pnas.1201830109

SI Methods

Materials. KnockOut DMEM (KO-DMEM), KnockOut serum replacement (KO-SR), basic fibroblast growth factor (bFGF), tumor growth factor β-3, L-glutamine, β-mercaptoethanol, nonessential amino acids solution (100×), penicillin-streptomycin solution (100×), Insulin-Transferrin-Selenium supplement (ITS; 100×), and Dulbecco's PBS (DPBS) were purchased from Invitrogen. Mouse embryonic fibroblasts were from Millipore. Porcine skin gelatin and tissue culture water were from Sigma-Aldrich. HyClone FBS, US origin was from Fisher Scientific. All other chemicals were purchased from Sigma-Aldrich unless otherwise noted.

Differentiation and Characterization of Mesenchymal Progenitors from hESC. hESC lines H9 and H13 were obtained from the WiCell Research Institute (Madison, WI) and expanded on mouse embryonic fibroblasts according to established protocols (Wicell Research Institute, Madison, WI; www.wicell.org). hESC expansion medium consisted of KO-DMEM supplemented with 20% (vol/vol) KO-SR, 5 ng/mL bFGF, 1 mM L-glutamine, 0.1 mM β-mercaptoethanol, and 0.1 mM nonessential amino acids.

Confluent cultures were switched to mesodermal medium consisting of KO-DMEM supplemented with 20% (vol/vol) HyClone FBS, 1 mM L-glutamine, 0.1 mM β-mercaptoethanol, 0.1 mM nonessential amino acids, and 100 U/mL penicillin/100 μg/mL streptomycin [1% (vol/vol) stock solution] for 7 d with two media changes. Induced cultures were trypsinized, counted, and subcultured in mesodermal medium at 100,000 cells per cm^2 on tissue culture plates coated with 0.1% (wt/vol) gelatin in tissue culture water (passage 1). Upon reaching confluence, cells were trypsinized and subcultured at 10,000/cm^2 for up to 55 d (up to 10 or 11 passages).

Cell growth was documented by counting cell numbers at each passage, and cell morphology was documented by light microscopy (microscope IX81 mounted with Q-imaging camera; Olympus) by using MetaMorph imaging software (Molecular Devices).

Expression of surface antigens was analyzed at passages 1, 3, 5, 7, and 10. Cells were suspended at 10^6 cells per mL, and 100 μL of the suspensions were incubated for 30 min on ice with antibodies Alexa Fluor 488 anti-human SSEA-1 (catalog no. 560172), Alexa Fluor 488 anti-human SSEA-4 (catalog no. 560308), Alexa Fluor 488 anti-human CD31 (catalog no. 558068), allophycocyanin anti-human CD34 (catalog no. 555824), fluorescein isothiocyanate anti-human CD44 (catalog no. 555478), phycoerythrin anti-human CD73 (catalog no. 550257), fluorescein isothiocyanate anti-human CD90 (catalog no. 555595), phycoerythrin anti-human CD166 (catalog no. 559263), and allophycocyanin anti-human CD271 (catalog no. 560326) obtained from BD Biosciences and Alexa Fluor 488 anti-human CD105 (catalog no. 323209) from BioLegend. Samples were washed and analyzed on the BD FACSAria system using the BD FACSDiva software (BD Biosciences).

Expression was compared with unstained controls and designated positive (+) when 70% or more of the population expressed the specific marker; weakly positive (+/−) when 20–70% of the population expressed the specific marker; and negative (-) when less than 20% of the population expressed the specific marker.

Differentiation potential of H9- and H13-derived mesodermal progenitors was evaluated in monolayers and pellet cultures at passage 4. In parallel, control differentiation cultures were prepared from two lots of human bone marrow derived mesenchymal stem cells (BMSC; Lonza) that were expanded to passage 4 in BMSC expansion medium (high glucose DMEM supplemented with 10% (vol/vol) FBS, 1 ng/mL bFGF, 0.1 mM nonessential amino acids, and 1% (vol/vol) stock solution penicillin/streptomycin).

For monolayer cultures, cells were seeded into 24-well cell culture plates and cultured for 3 wk in (*i*) control medium (DMEM supplemented with 10% (vol/vol) HyClone FBS and 1% (vol/vol) Pen-Strep), (*ii*) osteogenic medium (control medium, supplemented with 1 μM dexamethasone, 10 mM β-glycerophosphate, 50 μM ascorbic acid-2-phosphate, (*iii*) adipogenic induction medium [DMEM supplemented with 10% (vol/vol) HyClone FBS, 1% (vol/vol) Pen-Strep, 1 μM dexamethasone, 10 μg/mL insulin, 200 μM indomethacin, 500 μM 3-isobutyl-1-methylxanthine; days 1–7 and 15–21 after reaching confluence] and adipogenic maintenance medium (DMEM supplemented with 10% (vol/vol) HyClone FBS, 1% (vol/vol) Pen-Strep, 10 μg/mL insulin; days 8–14 after reaching confluence). Osteogenesis was evaluated by histological staining of alkaline phosphatase activity (Fast Blue RR Salt; Sigma-Aldrich) and mineralization staining by von Kossa. Adipogenesis was assessed by Oil Red O staining of accumulated lipids.

Cell pellets were prepared by centrifuging 3×10^5 cells $300 \times g$ for 5 min and incubated 4 wk in control medium, osteogenic medium, and chondrogenic medium (DMEM supplemented with 1% (vol/vol) Pen-Strep, 100 nM dexamethasone, 50 μg/mL ascorbic acid-2-phosphate, 40 μg/mL L-proline, 1 × ITS, 1 mM sodium pyruvate, 10 ng/mL tumor growth factor β-3). For histological evaluations, pellets were washed in PBS and fixed in 3.7% (vol/vol) formaldehyde (24 h at room temperature), mounted in Histogel (Fisher Scientific), embedded in paraffin, and sectioned at 5 μm. Mineralization was evaluated by von Kossa stain, the presence of glycosaminoglycans (GAG) was evaluated by Alcian Blue stain, and the amounts of GAG and calcium were determined biochemically.

Results of staining were documented by light microscopy under the same illumination, capture time, and white balance settings for differentiation and control conditions in each cell line (microscope IX81 mounted with Q-Color 3 imaging camera, Olympus) by using MetaMorph imaging software (Molecular Devices). Collected images from all cell lines were converted to the same size and resolution by using Adobe Photoshop and combined into a single figure by using Adobe Illustrator software.

Decellularized Bone Scaffolds. Bone disks (4 mm diameter × 4 mm high) were prepared as described (1, 2). Briefly, trabecular bone was cored into 4-mm-diameter plugs from the subchondral region of carpometacarpal joints of 2-wk- to 4-mo-old cows (Green Village Packing). The plugs were washed with high velocity stream of water to remove the marrow from the pore spaces, followed by sequential washes in PBS, hypotonic buffer, detergent, and enzymatic solution to remove cellular material. At the end of the process, decellularized bone plugs were extensively rinsed in PBS, freeze-dried, and cut to 4 mm of length to obtain scaffolds for cell cultivation. The dry weights and exact length of the plugs were measured and used to calculate the scaffold density and porosity. Scaffolds in the density range of 0.38–0.44 mg/mm^3 were sterilized in 70% ethanol and incubated in mesodermal medium overnight before cell seeding.

Construct Assembly and Perfusion Bioreactor Culture. H9 progenitors, H13 progenitors, and BMSC at passage 4 were suspended in culture medium at a density of 30×10^6 cells per mL, and a 40-μL aliquot of the cell suspension was pipetted into the blot-dried

scaffolds. Every 15 min, for 1 h, the scaffolds were flipped to facilitate uniform cell distribution. Each time, 5 μL of medium was added to prevent the cells from drying out. Seeded scaffolds were then placed in six well plates (1 scaffold per well) and incubated in 6 mL of osteogenic medium. The seeding efficiency, determined by evaluating the DNA content immediately after seeding, was between ∼60% for hESC progenitors (determined in three separate trials) and ∼80% for BMSC (similar to our previous studies). The initial cell density was determined before the transfer to bioreactors (day 3).

After 3 d, constructs were transferred to each of the perfusion bioreactors or six-well plates and cultured in osteogenic medium for up to 5 wk. Each bioreactor enabled uniform perfusion of six constructs, according to our established protocol (2). We selected a uniform flow rate of 3.6 mL/min corresponding to the interstitial velocity of 0.8 mm/s, which was set using a digital, low-flow, multichannel Ismatec peristaltic pump (Cole Palmer). These conditions were shown optimal in our previous work and close to settings used in other studies (2–4). Culture medium in the bioreactor was recirculated and maintained in equilibrium with the atmosphere in the incubator. These conditions established the oxygen concentration of 20% at the inlet of each construct. During culture, 50% of the medium volume was exchanged twice weekly with fresh medium. Medium samples were taken for biochemical assays at each medium change and stored at −80 °C. Cultured constructs were harvested after 3 and 5 wk of cultivation, cut in half, weighed, and processed for biochemical and histological analyses.

Implantation Assay. Safety and stability of H9-engineered bone constructs was assessed over 8 wk of s.c. implantation of cultured bone constructs in immunodeficient mice (SCID-beige female mice, 3–6 mo old; Harlan), according to an institutionally approved animal protocol. Controls consisted of (*i*) H9-derived mesenchymal progenitors seeded on scaffolds, (*ii*) undifferentiated H9 cells seeded on scaffolds, and (*iii*) undifferentiated H9 cells encapsulated in Matrigel.

Animals were allowed to acclimate before the surgery and were anesthetized with ketamine/xylazine. Two cell constructs per mouse were implanted into the dorsal s.c. pockets of three mice ($n = 6$ constructs per group). After 7–8 wk (after the tumors formed by undifferentiated cells in control groups reached a 5-mm diameter), mice were euthanized, and the tissues were harvested, washed, and fixed for μCT imaging and histological analyses.

Biochemical Analyses. For biochemical quantification of DNA and GAG content, samples were digested in 0.15 mL (pellets) or 1 mL (tissue constructs) of digestion buffer (10 mM Tris, 1 mM EDTA, and 0.1% (vol/vol) Triton X-100) containing 0.1 mg/mL proteinase K, overnight at 60 °C. Samples were repeatedly vortexed to facilitate digestion. Supernatants were collected and diluted as necessary to work in the linear range of the assays. DNA content was determined by using PicoGreen assay according to the manufacturer's protocols (Invitrogen). GAG content was determined from aliquots of the digest by using the 1,9-dimethylmethylene blue dye binding (DMMB) assay (5).

For determination of calcium content, pellets were extracted by incubation in 0.15 mL of 5% (vol/vol) trichloroacetic acid (Sigma) in water for 30 min with repeated pipetting, and the supernatants were analyzed by using Calcium (CPC) Liquicolor assay according to the manufacturer's instructions (Stanbio Laboratory).

For determination of alkaline phosphatase activity, tissue constructs were placed in 1 mL of lysis buffer [PBS, 1% (vol/vol) Triton X-100, 0.5% (wt/vol) sodium deoxycholate, 0.1% (wt/vol) SDS, 0.1 mg/mL phenylmethylsulfonylfluoride, and 0.3% (vol/vol) aprotinin], maintained on ice, and disintegrated by steel balls in a Minibead beater (Biospec) over two 15-s cycles. The extracts were collected, centrifuged, and 50 μL of the supernatant was incubated in 50 μL of alkaline buffer and 50 μL of nitrophenyl-phosphate substrate solution, in microcentrifuge tubes at 37 °C until the development of yellow color. The reactions were stopped with 0.5 M NaOH, and the reaction times were noted. The absorbance at 405 nm was compared with a standard curve obtained from p-nitrophenol solutions of known concentrations to determine the alkaline phosphatase activity.

Aliquots of culture medium were evaluated for the concentration of osteopontin, using a human osteopontin ELISA kit developed according to the manufacturer's instructions (R&D Systems).

Histological Analyses. Constructs were washed in PBS, cut in half, and fixed in 10% formalin for 1 d. One-half of each construct was processed for histological and immunohistochemical analysis by decalcifying for 2 d with Immunocal solution (Decal Chemical), dehydration in graded ethanol solutions, paraffin embedding, sectioning to 5 μm, and mounting on glass slides (2–5 samples were prepared for each experimental group and time point). Samples were stained by using routine hematoxylin/eosin and Masson trichrome procedures.

For evaluation of bone matrix, immunohistochemical staining was performed by using primary antibodies (all purchased from Millipore) against osteopontin (rabbit polyclonal anti-osteopontin, catalog no. AB1870), bone sialoprotein (rabbit polyclonal anti-BSP II, catalog no. AB1854), osteocalcin (rabbit polyclonal anti-osteocalcin, catalog no. AB10911), and human nuclear antigen (mouse monoclonal anti-HNA, catalog no. MAB1281). Tissue sections were deparaffinized with Citrisolv (Fisher Scientific) and rehydrated with a graded series of ethanol washes. The antigens were retrieved by incubation in citrate buffer, according to the manufacturer's protocols. The sections were then blocked with normal serum and stained with primary antibodies overnight, followed by the secondary antibody incubation, development with a biotin/avidin system, and counterstaining with hematoxylin. The serum, secondary antibody, and developing reagents were obtained from Vector Laboratories Vector Elite ABC kit (universal) (PK6200) and DAB/Ni Substrate (SK-4100). Negative controls were performed by omitting the primary antibody incubation step.

For hard-tissue histology, samples were fixed in 10% formalin (1–2 d) and dehydrated with sequential washes in ethanol (2 d at 70%, 2 d at 100% ethanol with twice daily solution changes) and toluene (2 d with once daily solution change). Subsequently, the samples were washed in activated methylmethacrylate (MMA) with daily changes of MMA solution for 4 d at 4 °C and then placed at 32 °C until the MMA was cured. Plastic-embedded sections were sectioned at 8 μm by using a Leica hard-tissue microtome. Osteoid formation was evaluated by the traditional Goldner's Masson trichrome staining.

Results of histological and immunohistochemical staining were documented by light microscopy under the same illumination, capture time, and white balance settings for all culture groups and negative staining controls (microscope BX53 mounted with DP72 camera; Olympus) by using DP2-BW imaging software (Olympus). Collected low-magnification images of hematoxylin/eosin, Masson trichrome, and immunohistochemical stains were processed in Adobe Photoshop to produce complete cross-section views of the tissues: Image levels were adjusted from 0–255 to 30–210 to enhance the contrast for viewing (except for osteocalcin and Masson trichrome), manually overlayed, and the top image brightness was adjusted (between 5 and 40) to minimize the differences in the border area. Images were merged, cropped to the same final canvas size for all groups, and combined into figures by using Adobe Illustrator. High magnification images of Masson trichrome and Goldner trichrome stains (with no level adjustments), hematoxylin/eosin stains (with levels adjusted to 30–240), human nuclear stains (with levels adjusted to 30–255), and immunohistochemical stains (with levels adjusted to 30–210)

were cropped to the same final canvas size for all groups by using Adobe Photoshop and combined into figures by using Adobe Illustrator.

Semiquantitative analyses of the histological and immunohistochemical sections were conducted by using ImageJ software (National Institutes of Health). For bone marker stains, each image was converted to an RGB Stack and the green stack was used. Thresholding was performed by using a value of 121 (selected based on the intensity of the negatively stained controls). Areas of the newly deposited tissue were manually selected, and the fractional area staining positive was measured for each sample in a complete cross-section. For osteoid stain, areas of positive (red) stain were manually selected, and the fractional area was measured for each sample.

μCT imaging. μCT was performed by using a modification of our developed protocol (6) on scaffolds before culture, in vitro cultured constructs, and explanted tissues. After fixation with glutaraldehyde, the samples were aligned along their axial direction and stabilized in a 15-mL centrifuge tube that was clamped within the specimen holder of a vivaCT 40 system (SCANCO Medical). The full 4-mm length of each construct was scanned at isotropic 21-μm resolution. The total bone volume (BV), consisting of the matrix in the scaffold and the new mineralized bone, was obtained by a global thresholding technique that selectively detects only the mineralized tissue. The bone volume fraction (BV/TV) was calculated by dividing the BV by the total volume of the sample. Spatial resolution of this full voxel model was considered sufficient for evaluating the microarchitecture of the bone tissue samples.

Statistical Analyses. Multiway analysis of variance (ANOVA) was used to compare different groups at the same time point and to compare different time points for any given group. Tukey's post hoc analysis and the STATISTICA software were then applied to individual comparisons, with $P < 0.05$ being considered as significant.

1. Grayson WL, et al. (2008) Effects of initial seeding density and fluid perfusion rate on formation of tissue-engineered bone. *Tissue Eng Part A* 14:1809–1820.
2. Grayson WL, et al. (2011) Optimizing the medium perfusion rate in bone tissue engineering bioreactors. *Biotechnol Bioeng* 108:1159–1170.
3. Holtorf HL, Jansen JA, Mikos AG (2005) Flow perfusion culture induces the osteoblastic differentiation of marrow stroma cell-scaffold constructs in the absence of dexamethasone. *J Biomed Mater Res A* 72:326–334.
4. Sikavitsas VI, Bancroft GN, Holtorf HL, Jansen JA, Mikos AG (2003) Mineralized matrix deposition by marrow stromal osteoblasts in 3D perfusion culture increases with increasing fluid shear forces. *Proc Natl Acad Sci USA* 100:14683–14688.
5. Farndale RW, Buttle DJ, Barrett AJ (1986) Improved quantitation and discrimination of sulphated glycosaminoglycans by use of dimethylmethylene blue. *Biochim Biophys Acta* 883:173–177.
6. Liu XS, Sajda P, Saha PK, Wehrli FW, Guo XE (2006) Quantification of the roles of trabecular microarchitecture and trabecular type in determining the elastic modulus of human trabecular bone. *J Bone Miner Res* 21:1608–1617.

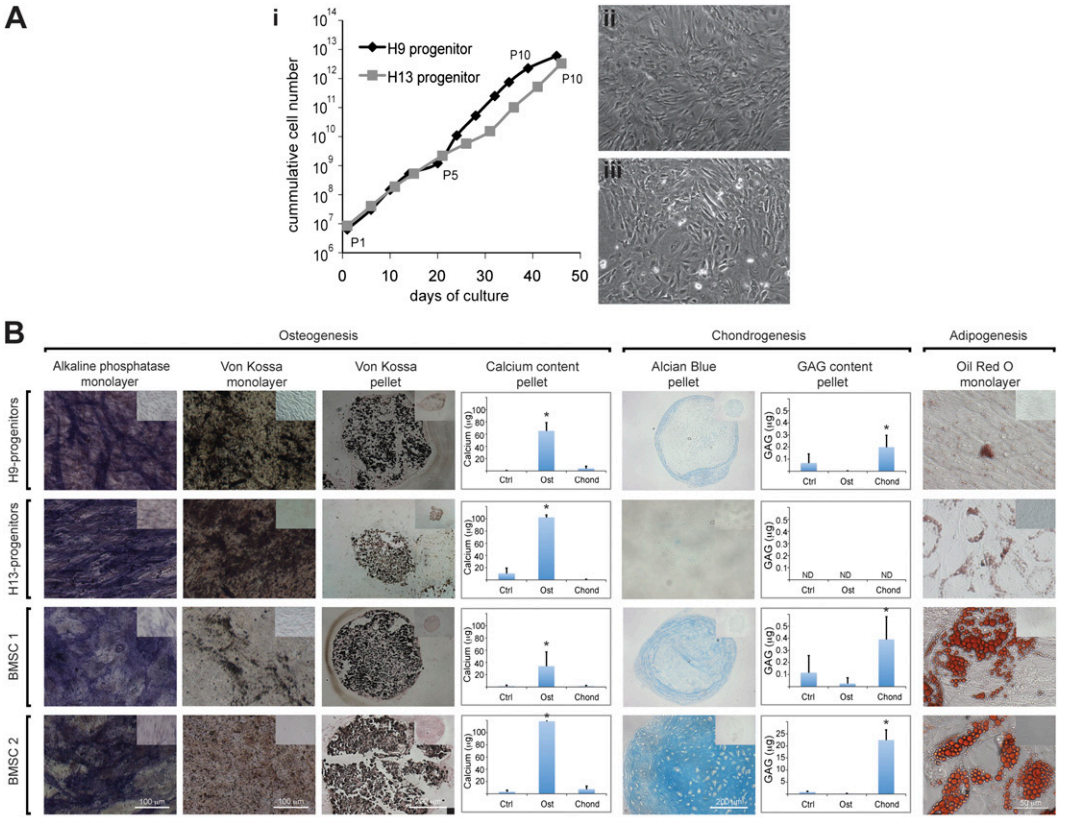

C

Surface antigen	H9-progenitor					H13-progenitor				
	P1	P3	P5	P7	P10	P1	P3	P5	P7	P10
SSEA-1	-	-	-	-	-	-	-	-	-	-
SSEA-4	-	-	-	-	-	-	-	-	-	-
CD31	-	-	-	-	-	-	-	+/-	-	-
CD34	-	-	-	-	-	-	-	-	-	-
CD44	+	+	+	+	+	+	+	+	+	+
CD73	+	+	+	+	+	+/-	+	+	+	+
CD90	+	+	+	+	+	+	+	+	+	+
CD105	-	+/-	-	+/-	-	-	-	+/-	+	+
CD166	+	+	+	+	+	+/-	+	+	+	+
CD271	-	-	-	-	-	-	-	-	-	-

Fig. S1. Characterization of the hESC-derived progenitors used in experiments. (*A*) Growth and morphology of hESC-derived progenitors. Adherent progenitors, derived from H9 and H13 lines, exhibited continuous growth for up to 10 passages (*i*) and exhibited fibroblastic morphology (*ii*, H9; *iii*, H13). (Magnification: 100×.) (*B*) Mesenchymal differentiation potential of hESC-progenitors and BMSC. H9- and H13-progenitor potential for osteogenesis was evidenced by positive staining of alkaline phosphatase activity (purple) in monolayer cultures and by matrix mineralization (von Kossa staining, black) in monolayer, and pellet cultures were stimulated with osteogenic medium (*Insets*, cultures in control medium). Mineralization was confirmed by biochemical evaluation of the pellet calcium content, which was significantly increased in osteogenic medium (Ost) compared with control (Ctrl) and chondrogenic (Chond) media. Osteogenesis of hESC-derived progenitors was comparable to that of BMSC. Weak chondrogenic potential was detected in H9-progenitor pellets compared with BMSC pellets by positive staining of glycosaminoglycanes (Alcian Blue) and by determination of glycosaminoglycans content, which was significantly increased in chondrogenic medium. Similarly, weak adipogenic potential of hESC-progenitors compared with BMSC was observed by positive staining of lipid vacuoles (Oil Red O) in monolayer cultures stimulated with adipogenic medium. Biochemical data represent averages of 3–6 measurements ± SD ($P < 0.05$; *, a statistically significant difference from other groups). (*C*) Surface antigen expression pattern of hESC progenitors. Expression at specific passage was designated positive (+) when 70% or more of the population expressed the specific marker; expression was designated weakly positive (+/–) when 20–70% of the population expressed the specific marker; expression was designated negative (-) when less than 20% of the population expressed the specific marker.

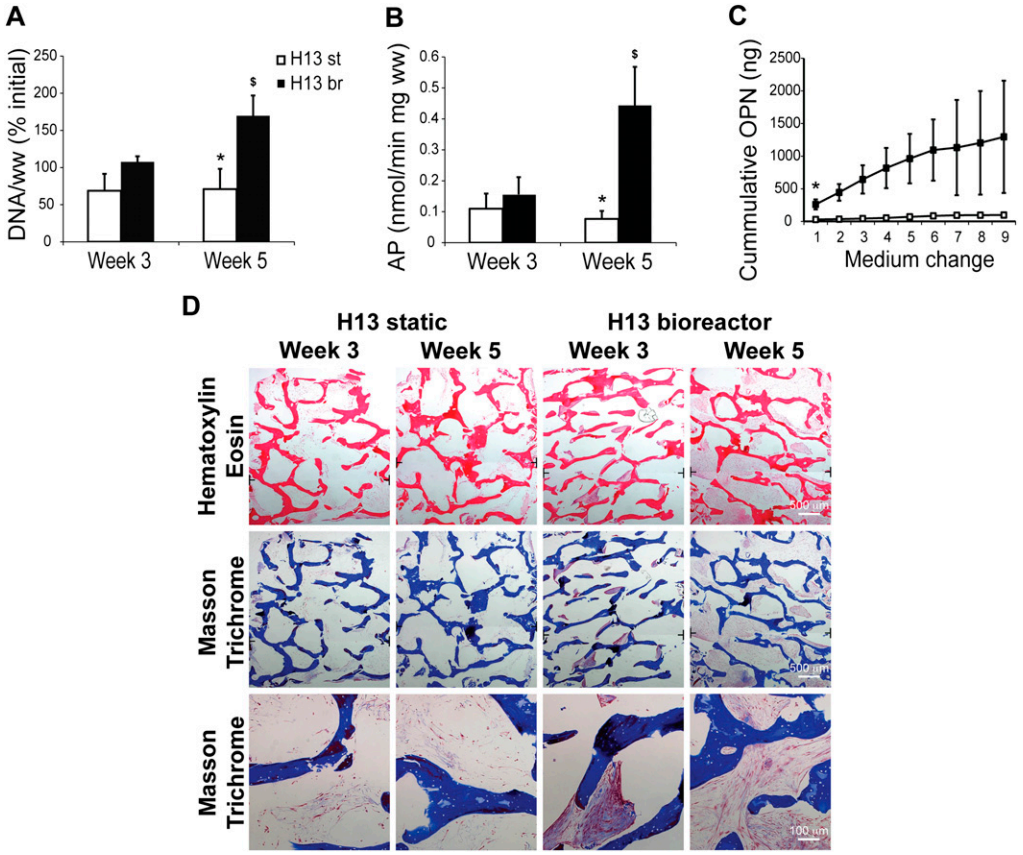

Fig. S2. Effect of bioreactor cultivation on tissue development from H13 progenitors. Both DNA content per ww (*A*) and AP activity (*B*) significantly increased in the bioreactor group from week 3 to week 5 of culture and were found to be significantly higher compared with the static group after 5 wk of culture. Cummulative osteopontin (OPN) release into culture medium was significantly higher during the first week of culture (medium change 1) and remained high compared with the static group throughout the culture (*C*). Data represent averages of 2–4 measurements ± SD ($P < 0.05$; *, a statistically significant difference between the groups; $, a statistically significant difference between week 3 and week 5). Positive effects of bioreactor culture were corroborated by histological analyses (*D*), showing denser tissue deposition in the bioreactor group and the presence of collagenous matrix (positive Masson Trichrome staining). Black T lines at the image edges mark the position where low magnification micrographs were overlayed.

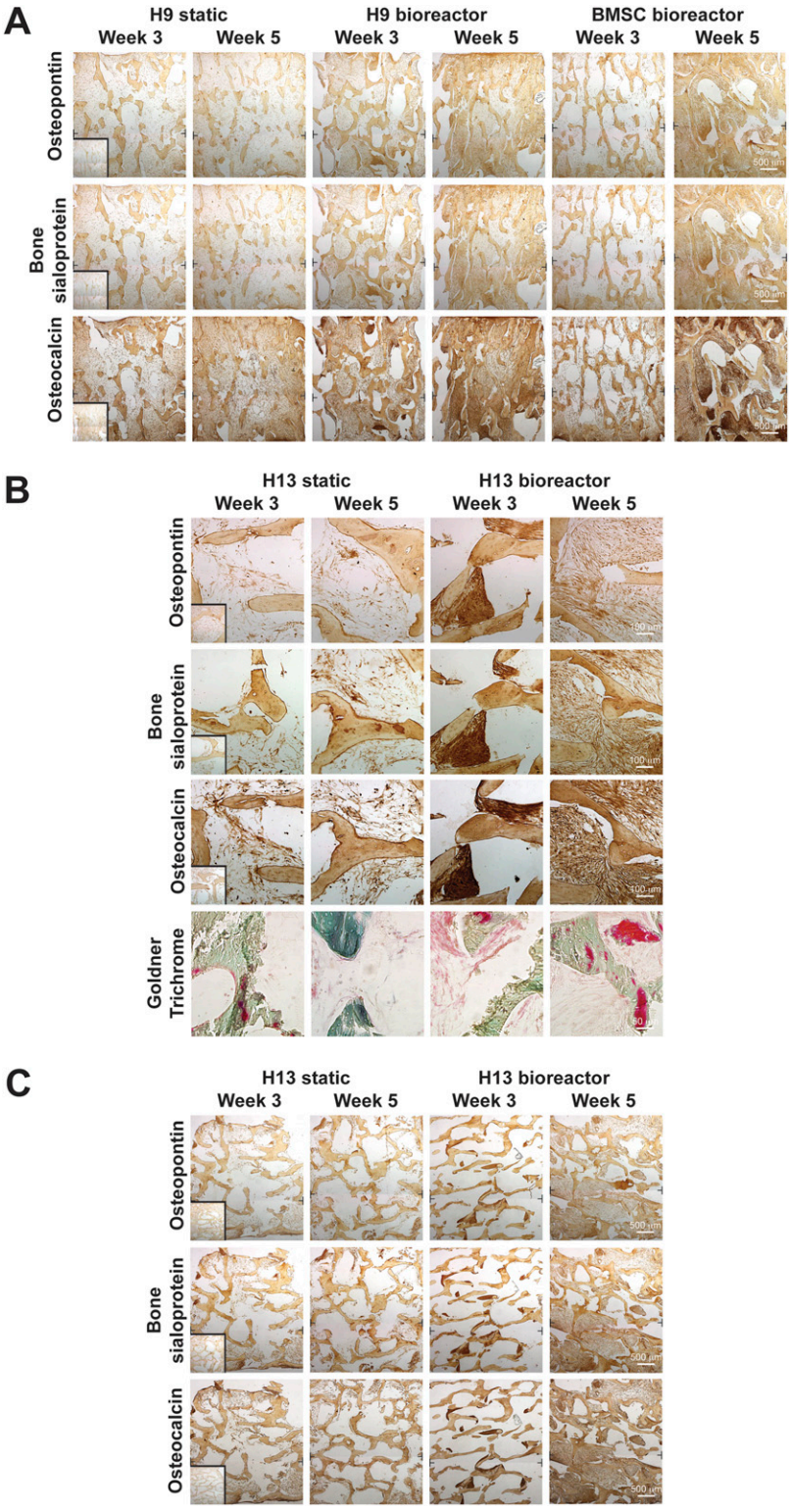

Fig. S3. Expression of bone markers in tissue constructs engineered using H9 progenitors, H13 progenitors, and BMSC under static and perfusion conditions. (*A*) Low magnification images showing homogenous expression of bone markers in engineered tissue. Bioreactor-engineered tissue from H9-progenitors and BMSC stained strongly positive for bone markers ostepontin (*Top*), bone sialoprotein (*Middle*), and osteocalcin (*Bottom*). *Insets* represent negative staining controls. Black T lines at the image edges mark the position where micrographs were overlayed. Minimal staining was observed in statically cultured groups at weeks 3 and 5. Interestingly, after 3 wk of culture, less homogenous matrix deposition was noted in BMSC compared with H9-progenitor bioreactor cultures. (*B*) Expression of bone markers in engineered tissue from H13 progenitors. Bioreactor-engineered tissue from H9 progenitors stained strongly positive for bone markers ostepontin (*Top*), bone sialoprotein (*Upper Middle*) and osteocalcin (*Lower Middle*). *Insets* represent negative staining controls. Minimal staining was observed in statically cultured groups at weeks 3 and 5. New osteoid deposition (*Bottom*; red color) was noted in both groups after 3 wk, and in the bioreactor group after 5 wk of culture. (*C*) Low magnification images showing expression of bone markers in engineered tissue from H13 progenitors. Bioreactor-engineered tissue from H13

Legend continued on following page

progenitors stained strongly positive for bone markers ostepontin (*Top*), bone sialoprotein (*Middle*) and osteocalcin (*Bottom*). *Insets* represent negative staining controls. Black T lines at the image edges mark the position where the micrographs were overlayed. Minimal staining was observed in statically cultured groups at weeks 3 and 5. Interestingly, after 3 wk of culture, dense and less homogenous matrix deposition was noted in bioreactor cultures compared with 5 wk of culture.

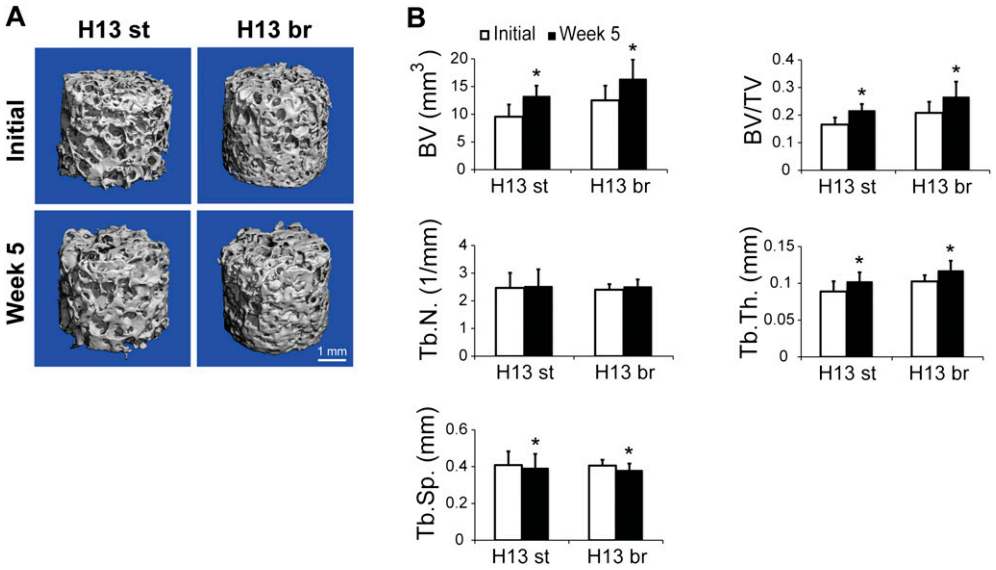

Fig. S4. Engineered bone mineralization. Reconstructed 3D μCT images of the tissue engineered bone constructs from H13 progenitors before and after 5 wk of cultivation indicated formation of mineralized tissue (*A*). Bone structural parameters were determined by μCT analysis and indicated bone maturation during in vitro culture (*B*). Bone volume, bone volume fraction, and trabecular thickness increased significantly in both groups, in contrast to trabecular spacing, which decreased significantly in both groups, indicating bone maturation. Data represent averages ± SD (n = 3–4, $P < 0.05$; *, statistically significant differences from initial values within the same group).

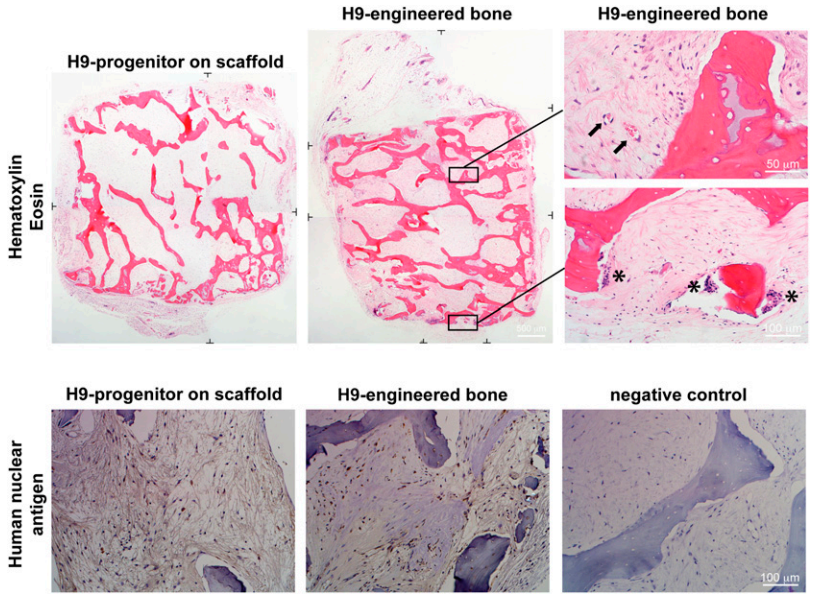

Fig. S5. Close examination of engineered bone tissue after explantation. Scaffold seeded with H9 progenitors and H9-engineered bone exhibited loose connective tissue and denser bone-like tissue upon closer examination. Explanted samples were surrounded by loose connective tissue capsule. Black T lines at the image edges mark the position where low magnification micrographs were overlayed. At higher magnification (*Top Right*), the presence of functional microvessels containing red blood cells was evident in the edge and interior regions of the scaffold (marked by arrows). In addition, external regions of the scaffolds indicated the initiation of remodeling process, evidenced by invasion of multinuclear osteoclastic cells overlaying and degrading scaffold surfaces (marked by asterisks). Brackets denote representative positions of high-magnification images. Human origin of the cells was confirmed by positive staining of human nuclear antigen (*Bottom*) both in scaffolds seeded with H9 progenitors as well as H9-engineered bone (brown color).